

Diphenylacetylene hydrogenation on a PdAg/Al₂O₃ single-atom catalyst: an experimental and DFT study

Aleksandr V. Rassolov, Dmitry Krivoruchenko, Michael G. Medvedev,
Igor S. Mashkovsky, Aleksandr Yu. Stakheev and Igor V. Svitanko

Selective alkyne hydrogenation

The liquid-phase hydrogenation of diphenylacetylene (98%, Aldrich) was performed at 25°C and an initial hydrogen pressure of 10 bar in *n*-hexane (98%, Merck) using an autoclave type reactor. The setup was equipped with a magnetic stirrer, a gas supply system, and a sampling unit. The amount of absorbed hydrogen was estimated from the pressure drop using an electronic pressure sensor. The catalyst amount and the intensity of mixing were selected in such a way as to be sure that the process runs in the kinetic region.¹

Selectivity to olefin formation ($S_{=}$) was calculated based on the data of the GC analysis of the reaction mixture:

$$S_{=} = n_{=}/(n_{=} - n.),$$

where $n_{=}$ and $n.$ are the mole fractions of the resulting olefin and alkane, respectively.

The reaction mixture was analyzed on a Crystal 5000 chromatograph equipped with a flame-ionization detector (Kchromatek, Russia). The mixture components were separated on an HP5-MS column (5% phenyldimethylsiloxane; 30 m × 0.25 mm ID with stationary phase film thickness 0.25 μm; and helium as carrier gas).

Transmission electron microscopy (TEM)

TEM analysis was performed on a Hitachi HT7700 (Japan) instrument. The optimization of microscopic measurements was carried out within the framework of an approach described earlier.² Before the measurements, powdered samples were supported from a suspension in

¹ P. V. Markov, G. O. Bragina, G. N. Baeva, O. P. Tkachenko, I. S. Mashkovsky, I. A. Yakushev, N. Yu. Kozitsyna, M. N. Vargaftik and A. Yu. Stakheev, *Kinet. Catal.*, 2015, **56**, 599 (*Kinet. Katal.*, 2015, **56**, 591).

² V. V. Kachala, L. L. Khemchyan, A. S. Kashin, N. V. Orlov, A. A. Grachev, S. S. Zalesskiy and V. P. Ananikov, *Russ. Chem. Rev.*, 2013, **82**, 648 (*Usp. Khim.*, 2013, **82**, 648).

isopropanol onto copper gauzes 3 mm in diameter covered with a layer of carbon. The images were obtained in the transmitted electron detection mode (bright field imaging) at an accelerating voltage of 100 kV. The average size of metal particles and the particle size distribution were determined based on the measurement of 120–150 particles in the micrographs of different sections of the samples.

Diffuse Reflectance Infrared Fourier Transform Spectroscopy (DRIFTS)

Diffuse Reflectance Infrared Fourier Transform Spectroscopy (DRIFTS) was performed with Tensor 27 Bruker spectrometer. The sample compartment of the cell (collector from Harrick) was filled with the as prepared sample. The sample (~20 mg) was first re-reduced *in situ* in the flow of 5vol. % H₂/Ar (550°C, 1 h). Then, the cell was cooled to 50°C and purged with Ar. A background spectrum was recorded under Ar. Then a flow (30 cm³/min) of 0.5 vol. % CO/He was introduced and spectra were recorded at 50°C.

CO chemisorption

The relative palladium dispersion was determined by CO pulse chemisorption at 35°C using a ASAP 2020 Chemi (“Micromeritics”, USA) setup. Before measurement the catalyst was reduced under hydrogen flow at 400°C for 30 min. Then helium was purged and the sample was cooled till 35°C. The CO was pulsed over the reduced catalyst until the TCD signal from the pulse was constant. The volume of CO adsorbed on the metal was determined from the CO isotherms in the pressure range 100 – 500 mm Hg. The number of surface Pd atoms, the dispersion and the average particle size were calculated by the formulas of the standard procedure³, taking into account the Pd/CO sorption coefficients:

$$N_s = \frac{V \times n \times N_A}{22414}, \quad (1)$$

where N_s – number of Pd surface atoms, V – CO volume required to form a monolayer coating, sm³ (NC), n – stiochiometric adsorption coefficient Pd/CO, N_A – the Avogadro constant;

Dispersion (D , %) was calculated as follows:

$$D = \frac{V \times n \times M}{m \times w \times 224.14}, \quad (2)$$

³ G. Bergeret and P. Gallezot, in *Handbook of Heterogeneous Catalysis*, eds. G. Ertl, H. Knözinger, F. Schüth and J. Weitkamp, Wiley-VCH, Weinheim, 2008, vol. 8. p. 3298.

where m – catalyst weight, g; w – the weight percentage, %; M – atomic weight (Pd), g/mol.

Average particle size was calculated via formula:

$$d = 6 \times \frac{(V_m / a_m)}{D}, \quad (3)$$

where V_m – volume occupied by an atom in a metal, nm³, a_m – area occupied by a surface Pd atom, nm².

Kinetics of the reaction

The catalytic activity of the synthesized catalysts was estimated in terms of catalyst turnover frequency at the first (TOF₁) and second (TOF₂) stages of hydrogenation from the reaction rates at these stages (r_1 and r_2 , respectively). The reaction rates r (mol_{H₂} g_{Cat}⁻¹ min⁻¹) were calculated evaluating the rate of H₂ absorption from the slope of the rectilinear segments of hydrogen uptake versus reaction time curves. Taking into account that the process occurs in two stages (C≡C to C=C and C=C to C-C hydrogenation) the reaction rates were calculated for both of them: at 0.1-0.5 eq. H₂ absorption for the first stage (r_1) and 1.2-1.5 eq. H₂ absorption for the second stage (r_2). Due to the fact that part of Pd surface may be occupied by atoms of the second metal it is difficult to determine the number of surface Pd atoms for the bimetallic catalysts by electron microscopy. For this reason, TOF was calculated as the ratio of the number of converted substrate molecules (consumed H₂ molecules) to the total number of Pd atoms in the catalyst. More details can be found elsewhere.¹

DFT calculations

All four steps of the hydrogenation reaction represented on Fig. 4 were modelled using a flat model of catalyst surface shown on Fig. S1. Its geometry was pre-optimized at PBE0-D3/SBKJC level of theory and held frozen throughout the further calculations.

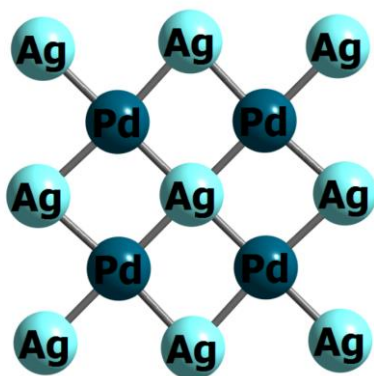


Figure S1 Flat model of catalyst surface.

The reaction was modeled as step-by-step hydrogenation of the substrate multiple bond, one hydrogen atom at time. At first, we aimed to get as good transition state guesses as possible. Therefore, we optimized the geometries of four manually-constructed initial TS guesses at the PBE0-D3/SBKJC level of theory in GAMESS-US with atoms H and C forming the novel bond being frozen. The PBE0 functional was chosen because it is known to be accurate for organic chemistry calculations and has recently been shown to be well-grounded in theory.

After convergence of the preliminary geometry optimizations, the Hessians were computed at the same level of theory and the actual searches for transition states were initiated at the PBE0-D3/SBKJC level of theory with QA optimization algorithm (maximum step 0.05 Bohr) using the calculated Hessians as initial guesses and updating them on each step using the POWELL method.

After convergence of the transition step searches, single-point energy calculations were performed at the PBE0-D3/IMCP-SR1 level of theory. The IMCP-SR1 basis set was chosen for the final energy evaluations as it incorporates scalar-relativistic effects, which are important for heavy elements, such as palladium and silver in our case, and belongs to model core potential basis sets which retain the correct nodal structures of atoms.

When the transition states were located, their imaginary frequencies were followed at PBE0-D3/SBKJC level of theory both forward and backward to locate corresponding starting and ending minima. Single-point energies in these minima were also computed with PBE0-D3/IMCP-SR1. Since the studied reactions are strictly successive, ending minima of one reaction is a starting one of another, so despite the different number of atoms considered for each transition state, we were able to calculate the relative energies for all steps. Importantly, our calculations benefit from a favorable error cancellation which rises from the fact that the studied TSs are very similar in nature, so systematic errors in them largely cancel out.

Normal modes analyses were performed for every located stationary point to verify them.

Computed structures are shown in Table S1.

Table S1 Computed structures and total energies.

